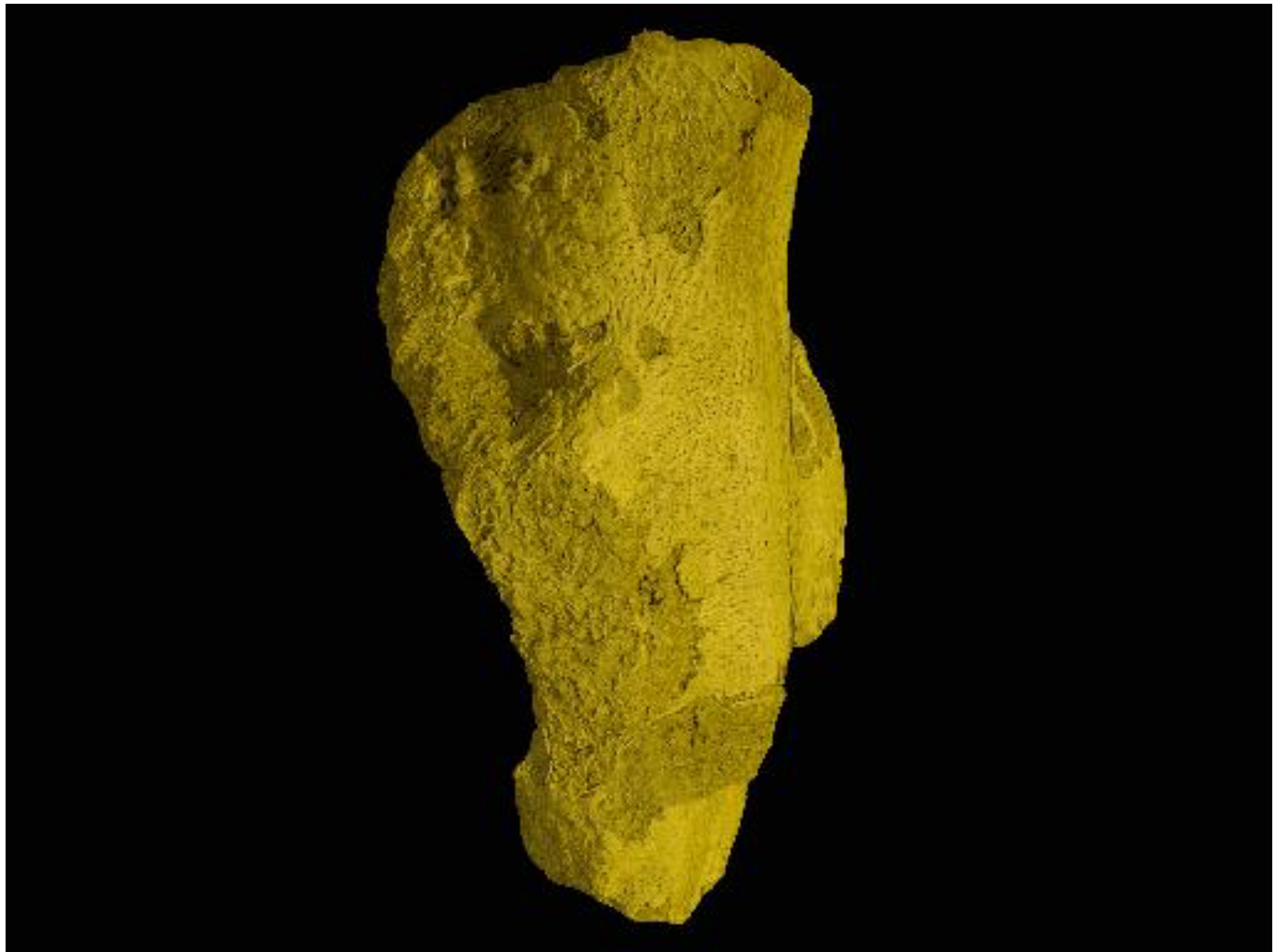


## SUPPLEMENTARY INFORMATION

### SUPPLEMENTARY MOVIE 1:

Movie showing the adult humerus of *Eusthenopteron*, illustrating the multiscale approach (from 20 $\mu\text{m}$  voxel size to 0.7  $\mu\text{m}$  voxel size).



## MICROTOMOGRAPHIC ACQUISITION PARAMETERS

- Acquisition parameters for bones of small extant animals:

The high-resolution scan ( $0.678\mu\text{m}$ ) of the humerus of *Desmognathus* was done using pink beam, with an energy of about 18.7keV, obtained thanks to the use of the undulator U17.6, whose gap was closed up to 16mm, and an aluminium filter of 0.25mm crossing the beam. The corresponding X-ray spectrum is presented in Supplementary Fig. 1. We used a propagation distance of 54mm between the sample and the detector to use the properties of the propagation phase contrast. The detector was a FreLoN 2K14 CCD camera (fast readout low noise) coupled to a GGG10 scintillator (Labiche et al., 2007; Martin et al., 2009). An objective 10x, N.A0.3 coupled with a 2X eyepiece was used in order to reach a pixel size of 0.678 microns. The scan was performed with 1500 projections in continuous rotation mode over 180 degrees with an exposure time of 0.2 seconds.

- Acquisition parameters for bones of small fossil animals:

The fossil samples scanned here, even if relatively small, remain too dense to be scanned at 18.7keV with pink beam. High-resolution scans of the fossil material were therefore performed with a single crystal 2.5nm period W/B4C multilayer monochromator, with energies ranging between 30 and 52keV (Supplementary Table 1). The propagation distance was selected to optimize contrast of the structures of interest. For the case of the interolateral region of *Compagopiscis*, we employed holotomography to increase the contrasts between structures of different densities. Holotomographic scans were performed using one scan for absorption (distance: 40mm) and two phase-propagation distances (85-210mm) at the energy of 40keV. The detector used was a FreLoN 2K14 or a FreLoN E2V CCD camera coupled with

different optical systems to adapt the resolution and efficiency to the purpose of each experiment (Labiche et al., 2007). Depending on the configurations, we took advantage either of the sensitivity but low speed of the FreLoN E2V CCD camera coupled with LSO scintillators, or of the higher speed, but lower efficiency of the FreLoN 2K14 CCD camera coupled with GGG scintillators (Martin et al., 2009). The different configurations we used are detailed in Supplementary Table 1. When the scans were performed over 180 degrees, 1500 projections were done; for a better signal to noise ratio, some scans were performed over 360 degrees with 1999 projections. When the scans were done in half-acquisition (scanning over 360 degrees with the center of rotation on one side of the picture), the width of the reconstructed slices could be increased up to 1.9 times the field of view; 5000 projections were therefore needed (corresponding to 2500 projections over 180 degrees on a virtual detector of 3900 pixels laterally). The time-exposure ranges between 0.5 and 2 seconds.

- Acquisition parameters for bones of big fossil animals:

The scan of the long bone of *Stenolaурhynchus* sp. was performed with pink beam at about 68.7keV. To reach this energy, the gap of the wiggler was closed up to 50mm and the beam was filtered with 2mm of aluminium, 0.25mm of copper and 0.25mm of tungsten. We used a Gadox scintillator of 5 $\mu$ m thick, and a FReLoN 2K14 CCD camera mounted on an optic delivering a pixel size of 5.06 $\mu$ m. The resulting pink beam spectrum is presented in Supplementary Fig. 1. The scan was done in phase contrast with a propagation distance of 4000mm. The long propagation distance leads to a small magnification of the picture due to the small beam divergence. The effective reconstructed voxel size was then 4.91 $\mu$ m. Such a voxel size is precise enough for a detailed observation of the vasculature. The scan was performed in half-

acquisition, continuous mode, over 360 degrees, with 5000 projections. The time of exposure was of 0.2 seconds.

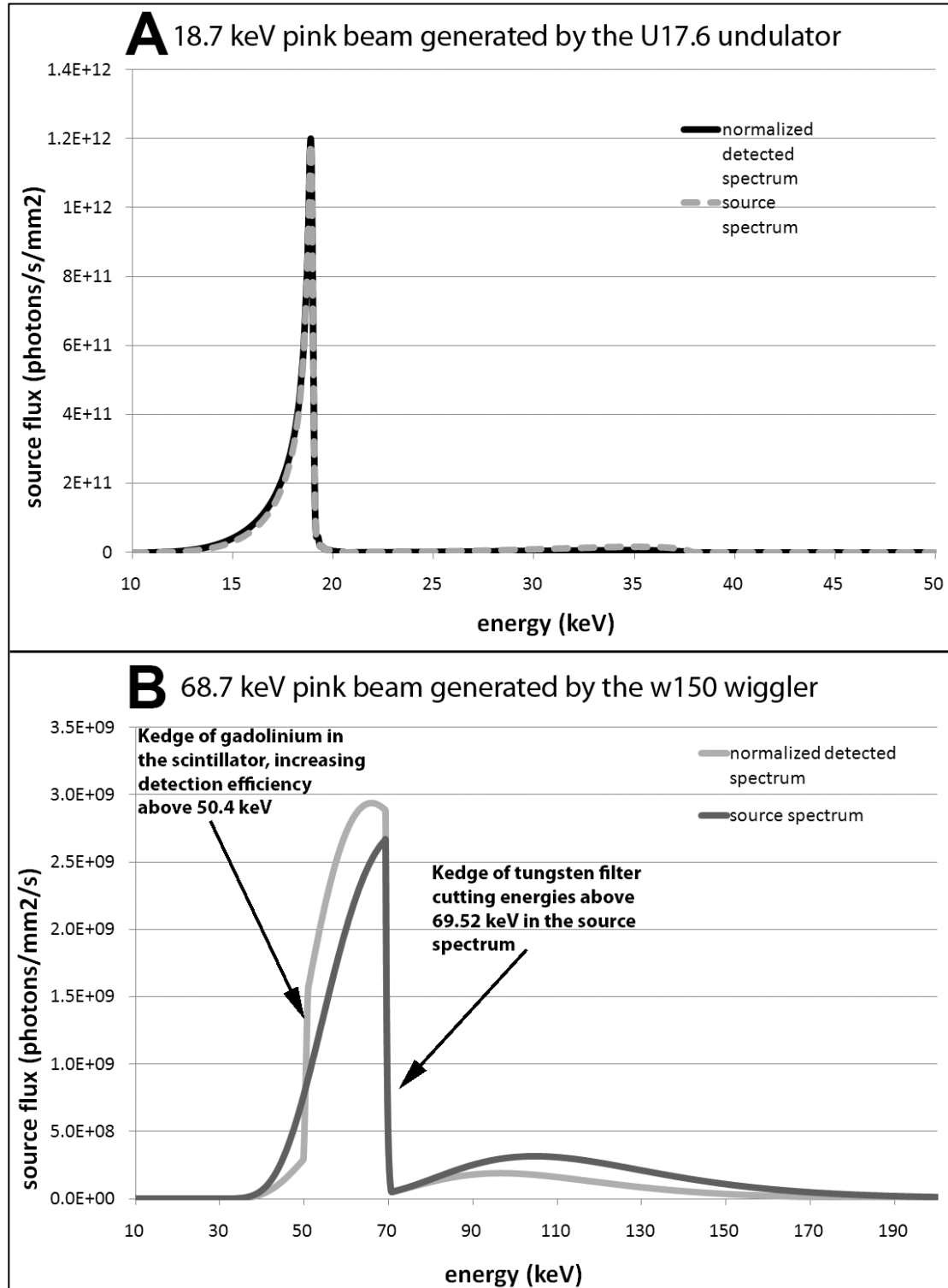
## REFERENCES

- LABICHE, J.-C., MATHON, O., PASCARELLI, S., NEWTON, M.A., GUILERA FERRE, G., CURFS, C., VAUGHAN, G., HOMS, A. & FERNANDEZ CARREIRAS, D. (2007). The fast readout low noise camera as a versatile X-ray detector for time resolved dispersive extended X-ray absorption fine structure and diffraction studies of dynamic problems in materials science, chemistry, and catalysis. *Review of Scientific Instruments* **78**, 091301-091311.
- MARTIN, T., DOUSSARD, P.-A., COUCHAUD, M., RACK, A., CECILIA, A., BAUMBACH, T. & DUPRÉ, K. (2009). LSO-based single crystal film scintillator for synchrotron-based hard X-ray micro-imaging. *IEEE Transactions on Nuclear Science* **56**, 1412-1418.

Scan name	Energy	Distances	Scan range	Projections	Count time	Voxel size	Camera / Scintillator	Decoheror
Compagopiscis_interolateral_musc_att_1	40	40, 85, 210	180	1500	0.7	0.678	2k14 / GGG10	no
0.7_Compagopiscis_1	40	50	360	1999	1	0.678	2k14 / GGG10	no
0.678_Eusthenop_juv_diap_dors_xc150	52	150	360	1999	2	0.678	2k14 / GGG10	no
0.678_Eusthenop_adult_dia_p_xc_150	52	150	360	1999	2	0.678	2k14 / GGG10	no
0.678_eusthenopteron_shoulder_girdle_ML_30_deco_xc50	30	5	180	1500	0.5	0.678	2k14 / GGG10	1mm
0.678_eusthenopteron_shoulder_girdle_ML_30_nodeco_xc50	30	50	180	1500	0.5	0.678	2k14 / GGG10	no
HA_0.75_Discauriscus_de_rmal_bone_second_test_OY_C	40	60	360 / HA	5000	0.7	0.744	E2V / LSO9	1mm

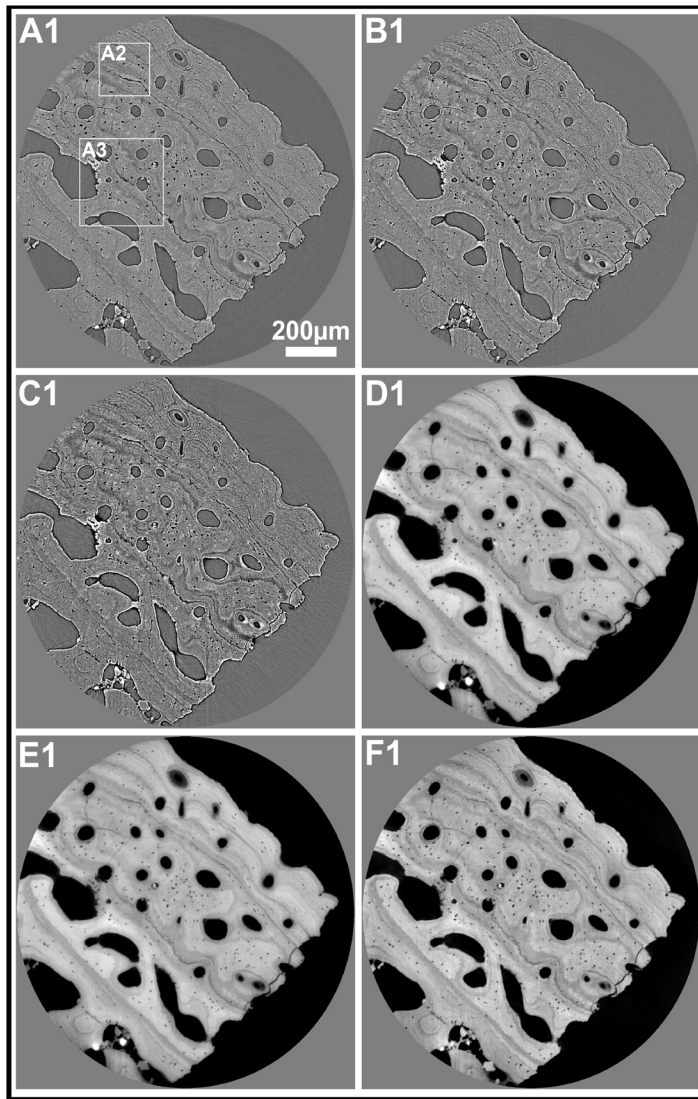
**Supplementary Table 1:** Acquisition parameters for scans done with a monochromatic beam. The first scan was done at three different distances for a holotomographic reconstruction.

## SUPPLEMENTARY FIGURE 1:



**Supplementary Figure 1:** Normalized detected spectrum and source spectrum for A/ the 'U17.6 configuration' and B/ the 'Wiggler' configuration.

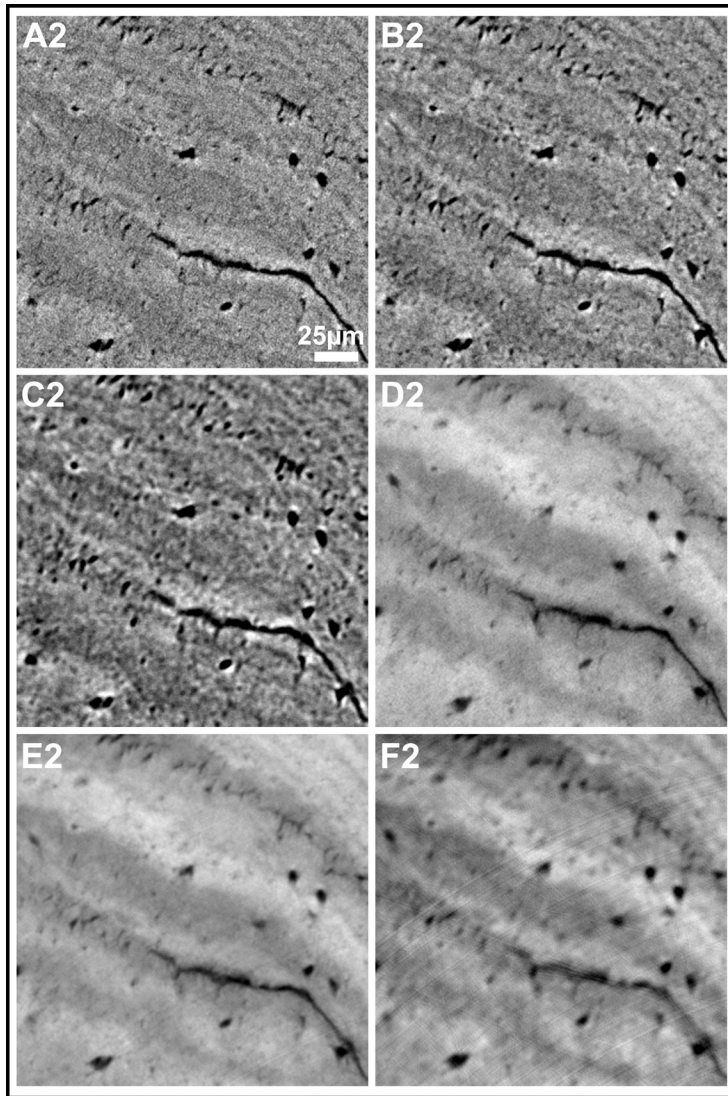
## SUPPLEMENTARY FIGURE 2:



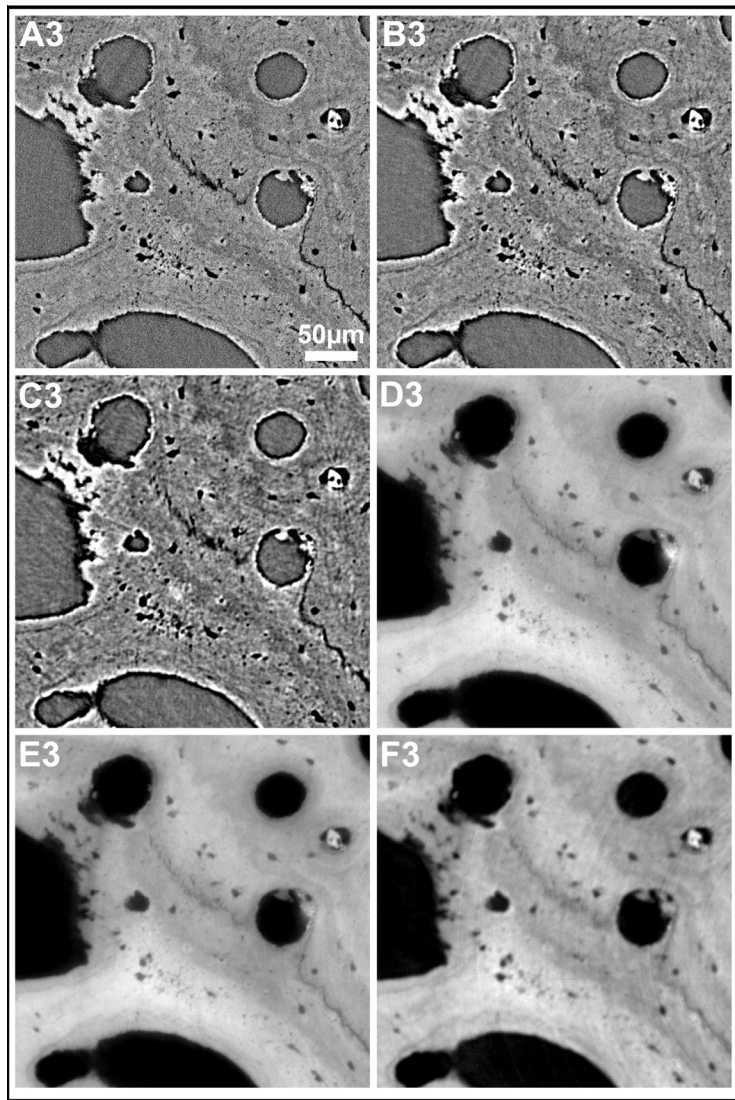
**Supplementary Figure 2\_1:** Comparative series of tomographic slices processed according to different methods at different propagation distances: A-C/ with edge detection; D-E/ with Paganin's approach; F/ as a holotomographic reconstruction; A, D/ with a propagation distance of 40mm; B, E/ with a propagation distance of 85mm; C/ with a propagation distance of 210mm. F/ The holotomography has been reconstructed from scans done at three distances: 40mm, 85mm, 210mm using a phase retrieval process adapted to absorbing samples like fossils (Guigay et al., 2007; Pradel et al., 2009). The same processing filters have been applied (ring correction and 3D unsharp mask). The value of delta/beta used for both Paganin's approach and the holotomography is the theoretical value for hydroxyapatite at 40keV: 706. A1-F1/ Full field of a view of a scan made in the interolateral plate of the placoderm *Compagopiscis* (voxel size: 0.678 $\mu$ m). A2, A3/ details shown in Supplementary Fig. 2\_2 and 2\_3.

### References

- GUIGAY, P., LANGER, M., BOISTEL, R. & CLOETENS, P. (2007). Mixed transfer function and transport of intensity approach for phase retrieval in the Fresnel region. *Optics Letters* **32**, 1617-1619.
- PRADEL, A., LANGER, M., MAISEY, J., GEFFARD-KURIYAMA, D., CLOETENS, P., JANVIER, P. & TAFFOREAU, P. (2009). Skull and brain of a 300 million-year-old chimaeroid fish revealed by synchrotron holotomography. *Proceedings of the National Academy of Sciences* **106**, 5224-5228.



**Supplementary Figure 2\_2:** Same comparative series of tomographic slices processed according to different methods at different propagation distances (for process details, see the caption of Supplementary Fig. 2\_1). A2-F2/ details of the corresponding region A2 (represented in Supplementary Fig. 2\_1) showing that the lines of arrested growth are sharper on the images processed with Paganin's approach than on the holotomographic data, despite extensive tests of holotomographic phase retrievals to improve the resolution of the phase maps.



**Supplementary Figure 2\_3:** Same comparative series of tomographic slices processed according to different methods at different propagation distances (for process details, see the caption of Supplementary Fig. 2\_1). A3-F3/ details of the corresponding region A3 (represented in Supplementary Fig. 2\_1) showing that submicron details (e.g., bone cell lacunae, extrinsic fibers) are sharper on the images processed with Paganin's approach than on the holotomographic data, despite extensive tests of holotomographic phase retrievals to improve the resolution of the phase maps.